Progression and stability analysis of rain forest tree growth under environmental stochasticity

DAVID M. NEWBERY† AND MARCUS LINGENFELDER

Institute of Plant Sciences, University of Bern, Altenbergrain 21, 3013 Bern, Switzerland

Abstract. Changes in relative stem growth rate (rgr) across periods of multi-censused plot data in tropical forest allow response indices (RIs) to be related to environmental (climatic) variation over time. Among small trees (12.5 to <50 cm girth at breast height [gbh]) in two permanent 4-ha plots at Danum, Sabah, Borneo (lowland dipterocarp formation), growth responses were followed before, during, and after a major ENSO drying event in 1998 (censuses of 1986, 1996, 1999, 2001, and 2007 in subplots). Overall, RI was negative in the interval with the drought, increased or reflected overcompensation in rgr immediately afterwards, and then settled back to pre-event levels. However, among the various tree species, responses and trajectories were very different: Some species showed positive or negative trends, while others showed stabilizing ones, and several had stable and unstable oscillations. Response index was graphed for pairs of periods in two ways: "consecutive" and "constitutive," allowing, respectively, progression (fundamental, implicit and explicit) and stability (fundamental, intended, and extended) to be examined. Strongest RIs were found among the understory species. Variation in RI was, nevertheless, very high between individuals within species and masked most average species' differences. Environmental stochasticity appears to lead to strong mixing effects of species composition over time, not necessarily randomly, but in a highly complicated manner depending on tree size, topographic location, neighborhood, and over–understory status, which would compound demographic stochasticity in recruitment to the small-tree class. Fluctuating responses cascade over one another in a highly unpredictable manner. These pluralistic responses may form the basis to a new understanding of tree population dynamics within the forest ecosystem, and to an improved theory about the maintenance of high species richness. Plasticity in allocation of resources to roots vs. shoots under water limitation offers a feasible hypothesis for high individual variation in growth. Instead of tropical rain forests being viewed as "complex," an empirically more sound way is to regard them as being highly "complicated" within a mechanistic and functional approach. Multi-species tree population dynamics are accordingly highly unpredictable and quasi-indeterminate.

Key words: Borneo; ENSO; lowland rain forest; tree responses; understory.

† **E-mail:** david.newbery@ips.unibe.ch

INTRODUCTION

Natural forests that persist over long periods of time are expected to show a dynamic equilibrium in the face of climatic perturbation, in terms of ecosystem structure, composition, and functioning, for which stabilizing mechanisms must by definition be operating. Establishing what these mechanisms are will enable a closer understanding of forest dynamics, and it will allow better informed and appropriate management where necessary. If the spectrum of perturbation has not changed greatly over recent millennia—what a particular forest experiences now is much

the same as what it likely did in the past—then the tree species found today exist, in part, because presumably they have adapted not just to the average environmental conditions of the site but also to its regime of climatic perturbation (Levins 1968, 1979).

Tree species may be expected to have evolved physiological mechanisms which enable them to accommodate the stresses caused by perturbations, and to recover from them; otherwise, stabilization could not be possible. Unless complete trait convergence has happened over evolutionary time, and is omnipresent, different species will respond in different ways and to differing degrees to create a *plurality* of responses (Newbery and Lingenfelder 2009). We posit that richness of tree species at a site is to a large part a consequence of this noisy mixing process. In this way, climatic perturbation, as an important component of environmental stochasticity affecting any forest, can be thought of as introducing extra "degrees of freedom" to the community, in a continually changing manner (Clark 2009, Clark et al. 2010).

While species-poor and simpler ecosystems—largely in the temperate regions—are also so affected, in the tropics it is quite possible that being species-rich under a noisy environment maintains or even promotes (together with other factors) that richness (Huston 1979, 1994). The forest suffers a stream of minor-to-moderate "interruptions," few of them necessarily so strong as to cause serious disturbances per se (i.e., major losses in biomass leading to succession) but enough to alter in finer ways the multitude of population interactions happening in time and space (Tokeshi 1999). In terms of species composition over time, in fact, the forest as a community would be expected to be in dynamic non-equilibrium, because species may change places with one another (completely or in varying proportions) under a host of random and non-random minor processes, yet filling up the guilds that enable the forest structure and overall function to continue. While demographic stochasticity is more aligned with biotic co-evolutionary processes, environmental stochasticity can be related more to structure and function overall, by way of physical tree species–climate interactions. These sources of stochasticity interact in highly complicated and almost unpredictable ways. For instance, how two species compete as neighbors will be influenced by their relative responses to the common perturbation, and vice versa (Newbery and Ridsdale 2016). If a top-down control is postulated, environmental stochasticity will mainly drive demographic stochasticity: If the opposite, then the converse will be the case.

Some tree species may be more or less resistant to perturbation, while others more or less resilient, with short- or long-term lags in recovery of their growth and population dynamics, also depending upon differences due to population structure and individual tree size, and the role of neighborhood competition. In a highly species-rich community, the number of varied patterns of response becomes multiplied up considerably (Lingenfelder and Newbery 2009, Newbery and Lingenfelder 2009). Some perturbations will occur relatively far apart (i.e., with low frequency) giving more time for recovery, while others relatively closer together (high frequency) giving less time for recovery. In the latter case, a forest mid-course in a recovery phase may be perturbed again—more or less strongly than it was previously. What for some decades may be a period of low frequency and then for some decades following one of high-frequency "averages out" to a value that hides the important effects of a few strong perturbations clustered in time once a century.

It is of interest to ask then: What is the minimum recovery time (the stabilizing period) in physical or physiological terms for a given ecosystem; is there evidence that species have been selected to respond sufficiently rapidly to avoid the set-backs of too-close-together perturbations—expressed in terms of their resilience; and do answers to this question depend on the relationship between a species' recovery potential and perturbation intensity? Given that by the end of the sapling stage and into the pole one (<3 cm diameter at breast height [dbh]), most of the biotic processes affecting seedling survival have played out (under the conditions of the contingent tree population), it is from this stage onward that tree growth per se involves responses to climatic perturbations, when crucially small trees begin to compete strongly with one another. It is at this very stage that an individual recruits in the strict sense of being a candidate to becoming incorporated into the forest stand, being part of the structure until old age. Furthermore, at this stage of

recruitment, silvicultural intervention is at its most effective (Vanclay 1994).

One way to assess the stability of a complex forest community is to follow individuals of the main species within a defined size class. This class offers a window on the life-cycle of the trees and their population dynamics. Small trees in the understory, those typically 10 to <50 cm girth at breast height (gbh) (1.3 m; or 3 to <16 cm dbh), have already survived the vagaries of dispersal, seedling establishment, and sapling growth, to become small trees or "poles" in the forest. They have not yet grown into the lower or mid-canopy, but onward recruitment into large size classes will follow. Further, in this size class of trees there is strong neighborhood competition occurs between individuals (Stoll and Newbery 2005, Newbery and Stoll 2013). Here, an important sorting of the species occurs (Newbery et al. 1992, 1999).

The understory is composed essentially of two groups of species: those where trees are truly understory and never grow so far as to attain large canopy sizes, and small trees of overstory some of which will grow onward and form the canopy or even emergents (Newbery et al. 1999). Such a labeling is heuristic because in reality a continuum exists with many inter-mediate-story positions. Nevertheless, the large majority (~85%) of trees in primary rain forest in the 10 to <50 cm class are understory (Newbery et al. 1992). In many managed forests in south-east Asia, after a first harvest, unwanted small trees of non-commercial value (those down to 15–45 cm gbh, Whitmore 1984), invariably mostly true understory species, are often removed in order to preferentially release pole trees for the next harvest. Likewise, during exploitation, much of this true understory is dis-regarded and therefore inevitably damaged. No recognition is usually made that these trees are an integral part of the forest system and that they may play an important role in future dynamics of the main canopy species (Newbery et al. 1992, 1999).

The present paper develops from the results of Newbery and Lingenfelder (2004, 2009) and is part two to Newbery et al. (2011). We attempt a stability analysis based on *empirical measures*, with no prior assumptions of stationarity or homoscedasticity (as in time-series analysis) or equilibrium and ergodicity (as in population matrix analysis). There is a large theoretical, and mostly speculative, literature on stability analysis of ecological communities, which is very largely untestable because (1) sufficiently long time series do not exist (or are unlikely to be available), and (2) communities are for the most not existing in any demonstrable state of equilibrium (May 1974). Any attempt to judge stabilizing mechanisms can only be possible for relatively short periods of time, and ideally, it should involve just one distinct perturbation. The basic physical responses of trees to pertur-bations suggest that natural selection will oper-ate on species' traits whatever the particular species. Different species' members of functional guilds can perform the same functions as others operating in a similar way (Loreau 2010). With a short window of time, no assumptions about past or future species composition can be securely made, although it is necessary to expect that the same mechanisms and traits will be operating in a similar manner over time.

We focus our analysis on tree growth rates since responses to the environment can be directly interpreted in physiological and physi-cal terms. Stability analysis in this context therefore follows the approaches of classical mechanistic physics. The motivation for the anal-ysis in this paper comes from earlier seminal work on environmental systems by Bennett and Chorley (1978: ch. 2). Growth rate is considered essential to population dynamics because, as a result of it changing, mortality, survivorship and longevity, maximum size and tree health, repro-ductive output, and hence recruitment are all strongly affected. The basic postulate is that growth rate response of small trees in the under-story and lower canopy—where competition for survival is most intense in a tropical forest—is a controlling pivotal process that allows ecosystem continuance in the face of environmental stochasticity. So while fluctuations due to envi-ronmental stochasticity are seen as the driving force, additional demographic stochasticity is subsumed in the analysis presented in this paper. This second force has considerable influ-ence on recruitment processes that occur before growth and survival ones operate within the small-tree size class. Growth rates, together with mortality rates, both being functions of tree size (i.e., stem diameter or girth) or age, enable the

demographic modeling of size-class frequency distributions over time under equilibrium and non-equilibrium conditions.

Given this set-up, it was expected that a drought perturbation to the whole forest would have a main effect on this small-size ("middle"-stage) class, the very small trees below <10 cm gbh being to a large degree protected and not competing because of their sparse spacing, and the much larger ones also not competing strongly with their deeper roots conferring resistance to water stress. The following questions were set: (1) Does the forest at Danum show stabilizing responses to perturbations among the common species? (2) How fast do the species recover from perturbation effects? (3) Do the current dynamics suggest a general mechanism that might be applied at longer time scales? (4) Do the results lead to a model of equilibrium or non-equilibrium dynamics? and, (5) is environmental stochasticity a plausible force for maintaining high species richness?

Study Site

The two main, permanent, long-term dynamics plots within the southeastern corner of the Danum Valley Conservation Area (117°48′ E, 4°58′ N), Sabah, Malaysia (N. E. Borneo), were established in 1985. The site is ~70-km inland of Lahad Datu on the coast. The plots are each 4 ha in area (100 × 400 m), positioned parallel to one another 280 m apart, and are lying on gently undulating terrain ~200–250 m a.s.l. Each has a topographic gradient from lower slope to ridge ranging over 35- to 40-m elevation (Newbery et al. 1996, Lingenfelder and Newbery 2009). The forest is primary lowland dipterocarp. There is clear evidence that the forest is in a late stage of successional recovery from a major drought event in the 1880s (Walsh and Newbery 1999), with continuing increase in basal area over recent decades, few and small gaps, and a very low density of pioneer species (Newbery et al. 1992, 1999). The two main tree families are the Dipterocarpaceae forming most of the overstory and the Euphorbiaceae dominating the understory. The equatorial climate at Danum is largely aseasonal, with a mean annual rainfall of 2832 mm (1986–2007) and a mean monthly temperature of 26.9°C (Newbery et al. 2011).

Methods

Field measurements

The first four complete enumerations of trees ≥10 cm stem gbh (or ≥3.2 cm diameter as dbh, normally at 1.3 m above the ground) in the two main 4-ha plots at Danum were made between (1) August 1985 and December 1986, (2) November 1995 and February 1997, (3) February 2001 and February 2002, and (4) March 2007 and February 2008. These are referred to as the 1986, 1996, 2001, and 2007 censuses, respectively: A fifth census has been completed recently (2014–2015), but its data are not used in the present analysis. The trees in the plots have been almost completely identified to the species level (Newbery et al. 1992, 1999). At each census, the gbh of every alive tree was measured: recorded status classified a tree as to whether it had died, recruited, or regressed (its gbh reduced to <10 cm) from the second census onward, or even recovered (grew back to ≥10 cm gbh) from the third onward. Using a set of codes for condition of stem (CoS) at point of measurement (PoM), and codes as to whether this PoM was renewed or had moved between successive censuses, allowed gbh measurements to be flagged as "valid" in the sense that their CoS and PoM statuses gave reliable and accurate girth increment estimates; conversely, any problematic trees were flagged as "invalid" (Lingenfelder and Newbery 2009). Mortality and recruitment are not considered in the present paper and are the subject of further work in preparation. After the major El Nino Southern Oscillation (ENSO) event in 1998 (Walsh and Newbery 1999, Newbery and Lingenfelder 2004, 2009, Fig. 1), sixteen 0.16-ha subplots, eight positioned in a stratified random manner over ridge and lower slope within each plot, were remeasured for just mortality of all trees and growth of small trees (those 10 to <50 cm gbh; Newbery and Lingenfelder 2004). The subplot measurements are referred to as the 1999 partial census. Subplots covered 2.56 of the 8 ha in all.

The data set

Average "valid" relative growth rates (rgr) of stems of small trees with 12.5 to <50.0 cm gbh (4.0 to <15.9 cm dbh) of the 48 most frequent species in the 16 subplots were found for each of the four periods: P_1 (1986–1996), P_{2a} (1996–1999), P_{2b}
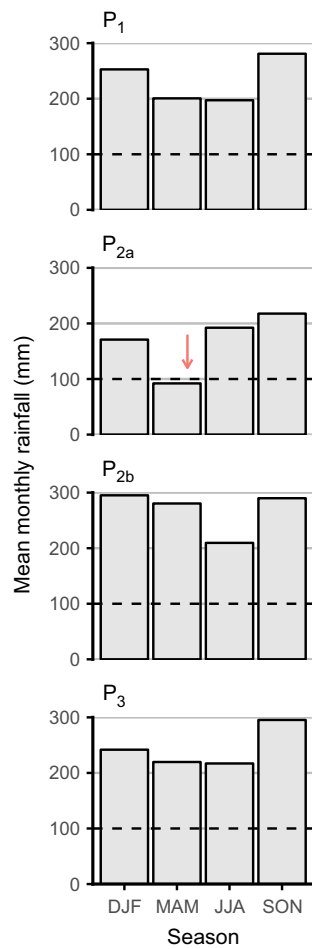
Fig. 1. Mean monthly rainfall (mm) at Danum during the four census periods P_1, P_{2a}, P_{2b}, and P_3 (from top to bottom), averaged across three-monthly seasons December–February, March–May, June–August, and September–November. The horizontal dashed line shows the assumed evapotranspiration threshold at 100 mm/month. The red arrow points to the minimum 30-d running total of rainfall and the maximum deficit in antecedent rainfall, during early May 1998 (see Newbery and Lingenfelder 2009).

(1999–2001), and P_3 (2001–2007), continuing with the notation of Newbery and Lingenfelder (2004, 2009), and Newbery et al. (2011). While this is a subset of all the data for trees ≥10 cm gbh in the whole plots at Danum, it (1) includes the partial census just nine months after the 1998 ENSO event, made only for small trees (10 to <50 cm gbh); (2) uses subplots that were randomly chosen in a stratified manner with respect to topography and were therefore spatially independent; and (3) focuses on the size class of trees, the smallest, for which stem gbh was measured the most accurately. Raising the minimum gbh to 12.5 cm removed any bias caused by the omission in recording of 1999 recruits (see Newbery and Lingenfelder 2004, Newbery et al. 2011). Numbers of trees in P_1, P_{2a}, P_{2b}, and P_3 were 2093, 2326, 2165, and 2153, respectively (total = 8737, mean density = 853 ha^{-1}).

Over–understory index

Newbery et al. (2011) reported on species gbh size-class distributions, in terms of numbers of trees and basal area abundance of them per gbh interval, and these measures were there combined to provide an over–understory index (OUI) for the 100 species with the highest density (both plots). Early forms of the index were already used in Newbery et al. (1992, 1999). The index ranges from 0 to 100 representing the extremes of under- and overstory habit. Species for which trees with gbh ≥ 30 cm make a low proportion of those ≥10 cm gbh (toward 0) in terms of number and basal area are more "understory" in habit, while those for which the proportions are high (toward 100) are more "overstory." The OUI values for the 48 species in the present analysis were adopted from that longer list. Following the analysis in Newbery et al. (2011), the 48 species were classified according to OUI and mean gbh into understory, intermediate, and overstory species (Appendix S1: Table S1).

Response index for growth

Response indices, RI_{i-j}, first developed as "RD" in Newbery and Lingenfelder (2009) for the immediate effect of the 1998 drought (i.e., for P_1, P_{2a}, and P_{2b} only), were found here in a more general form for the six possible pairs of successive periods (i, j) up to and including P_3, where $i = 1, 2, 3$ and $j = 2, 3, 4$ (1–4 corresponding to the four periods) using all of the rates per period for each species where t_i and t_j are the lengths of periods:

$$RI_{i-j} = \frac{(\mathrm{rgr}_j - \mathrm{rgr}_i) \cdot ((t_i + t_j) \cdot 100)}{(t_i \cdot \mathrm{rgr}_i) + (t_j \cdot \mathrm{rgr}_j)}.$$

The relative change (on a percent scale) is expressed as the difference in rgr between the

two periods considered, divided by the mean of the two rates where these are weighted by the lengths of their respective periods. P_1, P_{2a}, P_{2b}, and P_3 were taken as being of 10-, 2.5-, 2.5-, and 6-yr duration, respectively, values very close to their actual mean lengths (Newbery et al. 2011). While previous estimates of RI_{i-j} (=RD_{i-j}, Newbery and Lingenfelder 2009) used all small trees above the minimum gbh enumerated, that is, those 10 to <50 cm gbh, only 22 species were analyzed, and the recruitment bias was not catered for.

Changes in rgr from P_1 to P_3 form a set of three phases, with firstly a *reaction* to the perturbation in P_1 to P_{2a} (RI_{1-2a}), then *post-reaction 1* in P_{2a} to P_{2b} (RI_{2a-2b}), and *post-reaction 2* in P_{2b} to P_3 (RI_{2b-3}). Period P_{2a} is pivotal in the series because it contained the strong drought perturbation (Fig. 1). The effects of weighting period rates, as opposed to using averages in the denominator of RI_{i-j}, are compared in Appendix S1: Fig. S1 plotted against percentage change from the rate in the first period [i.e., $((rgr_j - rgr_i)/rgr_i) \times 100$]. The relationships are very similar and near to linear for the range ±50%, and close up to +100%, but where percentage increase is −100%, weighted and un-weighted RI_{i-j} values will be −150% and −200%, respectively (P_1 and P_2 compared). Weighting had a moderate linearizing effect overall.

Two aspects of rgr measurement and its use in RI_{i-j} need qualification. Firstly, the analysis of responses used valid growth rates. Trees that would have been damaged or dying likely had lower growth rates but these would have been excluded due to poor CoS (Lingenfelder and Newbery 2009). Secondly, rgr might have depended to some extent on gbh, even within the small-tree size class of 10 to <50 cm gbh. But since the formula for RI_{i-j} involves a difference (change) in rgr divided by weighted mean rgr, unless average gbh itself changed much between periods, gbh would have had little influence. For simpler rgr differences, Newbery et al. (2011) found gbh change to have minimal effects (App. B, loc. cit.).

Alternative forms of response

For comparison, two other versions of RI_{i-j} were calculated: Firstly, removing those trees with valid rates in a first period but which died in the second one, and likewise those trees recruiting into the second, but not present in the first period, allowed "matching" mean rgr_m values to be found, and their corresponding mRI_{i-j} values. Secondly, mean rgr_q values were found for just those trees in the upper quartile (q_1) of values per species, individually for each period, and these were then used to similarly provide qRI_{i-j} values. The mRI_{i-j} removed a "young-replacing-old" effect when comparing across periods: qRI_{i-j} gave emphasis to the most likely survivors in each period since these were the fastest growing trees per species. In the case of matching, mean values of rgr in a period changed slightly depending on the other period with which it was being compared.

Bootstrap and randomization tests

Mean estimates of RI_{i-j} for the 48 species × six pairwise combinations of periods were bootstrapped to find their 90% confidence limits (N = 2000) using the "bootstrap" procedure in GenStat version 15 (Payne et al. 2011). "Bootstrap" calls another procedure "resample" in which RI_{i-j} is calculated from the sampled rgr values in the relevant periods i and j. Agreement between the bootstrapped means for species and the empirical values in Table 1 was overall very close, except for three cases (of the 288 in all): In two other cases, limits were discounted because they were unrealistically very large (Appendix S1: Note S1).

Those species whose RI_{i-j} values differed significantly from what would be expected from complete randomization of all rgr values across trees (and thus species) were highlighted in the following way (after Newbery and Lingenfelder 2009). Using N = 2000 Monte Carlo simulations, the valid rgr values from all species in the plots (not just the 48 selected) were completely permutated, and the mean rgr per species was found (i.e., samples the same size as each species recorded). For the 48 species of interest, the percentiles of their N ranked values defined the 10%, 5%, 1%, and 0.1% confidence limits in RI_{i-j}. If the mean observed RI_{i-j} for a species lay outside of its limits (determined in part by population size), it was considered significant. This is not a formal test of a null hypothesis: It is a simple statistical guide to the more prominent differences.

Table 1. The response index RI_{i-j} (%) calculated pairwise for the successive periods i and j (see main text for formula), based on mean rgr of all valid rates per species.

Species	Code	OUI	n	RI_{1-2a}	RI_{1-2b}	RI_{1-3}	RI_{2a-2b}	RI_{2a-3}	RI_{2b-3}
Aglaia silvestris	Asi	37.9	20	−35.3	48.4	−15.9	78.4	22.5	−65.2
Alangium javanicum	Aj	21.9	17	−59.3	−11.2	−36.5	61.8	33.8	−28.6
Antidesma neurocarpum	An	0.3	15	−55.0	155.7†	136.3***	146.4*	116.3**	14.5
Aporosa falcifera	Af	54.1	51	−67.6**	−18.5*	−17.8	67.9	60.6	1.5
Ardisia sanguinolenta	Asa	6.8	95	−45.1†	11.9	−14.2	62.8	35.6	−27.3
Baccaurea tetrandra	Bt	40.8	46	−31.9	49.8	35.7	75.7	59.2	−9.7
Barringtonia lanceolata	Bl	60.4	22	−50.2	32.0	−12.4	84.6	43.1	−45.3
Buchanania insignis	Bi	17.8	29	20.2	−4.8	5.7	−23.9*	−13.8	10.3
Chisocheton sarawakanus	Cs	49.0	26	33.0	61.8	19.1	23.0	−11.8	−37.0
Cleistanthus contractus	Cc	3.0	71	−43.9	54.8	20.5	92.1†	60.2†	−29.4
Dacryodes rostrata	Dr	26.1	40	14.2	21.6	−6.1	6.7	−20.6	−27.8
Dehaasia gigantocarpa	Dg	15.6	28	−109.9***	12.8	5.9	167.8***	123.7***	−6.5
Diospyros elliptifolia	De	32.2	16	−4.5	−43.3	−32.0	−45.6†	−30.7	16.7
Dimorphocalyx muricatus	Dm	9.8	182	−5.4	145.0***	56.1***	105.1***	51.4*	−63.4**
Dysoxylum cyrtobotryum	Dc	50.2	31	−33.9	−2.7	−22.6	35.0	14.3	−21.4
Dysoxylum rigidum	Do	24.5	19	−18.7	40.1	−6.7	54.7	12.8	−46.3
Fordia splendidissima	Fs	4.0	89	−33.1	18.3	25.9	53.2	53.8	7.7
Gonystylus keithii	Gk	42.3	27	1.6	−2.3	16.0	−0.4	13.8	17.3
Hopea nervosa	Hn	31.1	16	3.5	22.2	−21.5	17.4	−26.9	−46.5
Hydnocarpus borneensis	Hb	10.6	21	−34.9	−67.0**	9.3	−48.9*	43.5	76.9***
Hydnocarpus polypetalus	Hp	22.0	30	−3.4	38.2	26.2	37.6	27.1	−9.3
Knema latericia	Kl	5.1	26	1.3	−7.9	−31.1	−9.4	−36.1	−25.7
Lithocarpus nieuwenhuisii	Ln	57.0	20	9.1	32.5	−19.3	20.9	−30.3	−54.1
Litsea caulocarpa	Lc	16.4	53	−5.3	48.1	53.0	47.2	49.2	8.0
Litsea ochracea	Lo	27.7	39	−48.7	−41.9***	−75.7***	9.8	−32.2†	−43.1
Lophopetalum beccarianum	Lb	18.3	45	8.0	50.6	−14.9	36.5	−24.0†	−66.1
Madhuca korthalsii	Mk	32.1	76	−3.5	18.3	−22.7†	20.9	−20.7*	−44.0
Magnolia candollei	Mca	9.1	22	−11.6	88.9	68.3	80.5	63.9	−8.3
Magnolia gigantifolia	Mg	6.1	18	0.4	5.0	−89.7***	4.5	−128.1***	−133.4*
Mallotus penangensis	Mp	19.4	40	11.6	47.7	−2.5	30.9	−14.1	−48.5
Mallotus stipularis	Ms	27.9	20	−51.9	130.7†	106.1*	135.8*	106.0***	−0.3
Mallotus wrayi	Mw	10.4	441	−14.1	72.2***	32.9***	72.5***	41.8*	−31.0
Maschalocorymbus corymbosus	Mco	0.8	50	−50.8	44.6	30.7	93.8†	72.9*	−10.2
Parashorea malaanonan	Pm	65.1	16	4.8	−28.6	−62.1†	−35.9	−83.9†	−41.3
Pentace laxiflora	Pl	63.0	24	−18.5	2.8	−23.3	22.3	−4.5	−28.2
Polyalthia cauliflora	Pca	11.9	83	−38.9	34.0	46.1†	72.5	71.3***	12.8
Polyalthia congesta	Pco	30.2	20	42.1	37.8	25.6	−3.5	−13.2	−9.5
Polyalthia rumphii	Pr	20.0	42	−1.8	109.6*	20.4	84.0	20.7	−75.5
Polyalthia sumatrana	Ps	44.0	32	−2.9	40.5	−23.9	38.9	−22.8	−67.7
Polyalthia xanthopetala	Px	14.9	28	−8.1	12.5	5.4	20.3	13.4	−6.8
Reinwardtiodendron humile	Rh	18.1	29	−75.5*	−21.6	5.9	79.1	84.3*	27.2
Shorea fallax	Sf	39.2	54	−64.1*	−27.7*	−8.2	52.3	62.9	21.1
Shorea pauciflora	Sp	65.8	19	28.1	−3.8	−62.0†	−29.7†	−109.3**	−73.4
Syzygium chrysanthum	Sc	37.5	15	101.5*	76.9	75.4	−17.4	−10.5	7.1
Syzygium elopurae	Se	23.2	26	11.8	28.2	16.4	14.7	4.6	−10.2
Syzygium lineatum	Sl	63.0	19	−0.1	−42.7†	−87.5***	−48.8*	−122.9***	−63.2
Syzygium tawaense	St	57.7	17	70.3	49.1	−9.9	−16.3	−77.9*	−58.6
Xanthophyllum vitellinum	Xv	28.6	26	−36.0	−1.7	66.6	38.7	80.1†	55.8*
rgr (all valid rates)									
Mean				−14.6	27.4	4.0	38.8	12.7	−22.6
SE				5.4	6.8	6.5	7.2	8.4	5.4
Min.				−109.9	−67.0	−89.7	−48.9	−128.1	−133.4
Max.				101.5	155.7	136.3	167.8	123.6	76.9

(Table. 1. Continued)

Species	Code	OUI	n	RI_{1-2a}	RI_{1-2b}	RI_{1-3}	RI_{2a-2b}	RI_{2a-3}	RI_{2b-3}
rgr_m (all, matched trees)									
Mean				−25.6	12.5	−10.0	33.6	2.2	−28.3
SE				5.4	7.1	6.8	6.7	8.4	5.4
Min.				−131.2	−97.8	−93.0	−76.6	−158.1	−143.2
Max.				82.2	146.3	140.3	166.2	124.8	62.9
rgr_q (top quartile rates)									
Mean				7.4	42.9	10.8	29.8	0.5	−28.9
SE				4.9	6.7	6.0	5.5	6.8	4.6
Min.				−60.9	−27.9	−63.9	−44.8	−116.1	−88.6
Max.				114.8	184.3	136.4	117.3	88.7	52.1

Notes: OUI, over–understory index (see text for explanation); SE, standard error. Below the main table are the RI_{i-j} summary statistics, the summary statistics for RI_{i-j} based on tree-matched rgr values (rgr_m), and the mean rgr in the top quartile of valid rates (rgr_q). The "†" and "*" symbols indicate statistical significance according to the permutation tests. n is the average number of trees across the four censuses.

***$P \le 0.01$; **$P \le 0.01$; *$P \le 0.05$; †$P \le 0.10$; otherwise *ns*, $P > 0.10$.

Regression analysis under permutation

To test whether relationships between pairs of RI_{i-j} values differed significantly from what might be expected under null hypotheses, standardized major-axis regressions (SMA, Legendre and Legendre 1998: 504–516) were fitted across the 48 species for the observed data and for N = 2000 random permutations of the rgr values that were the basis to each RI_{i-j} variable (Roff 2006). For these eight tests, the rgr variable that was common to the two RI_{i-j} values in the pair under consideration was held unchanged and the other rgr variable was permutated (see Appendix S1: Table S2 for details; calculations made in a Fortran95 program). Ordering the N values enabled confidence limits that excluded the most extreme 10%, 5%, 2%, and 1% values to be defined. Permutation tests were rerun for each of three groups of species, those of the under-, intermediate, and overstories. The major-axis regression employed standardization of the variables because different RI_{i-j} variables had different ranges depending on their interval weightings: Fitted coefficients were accordingly de-standardized.

RESULTS

Responses

Mean RI_{i-j} shifted from −15% for P_1–P_{2a} to 27% for P_1–P_{2b} and resolved to near zero (4%) for P_1–P_3. Likewise, the mean RI_{i-j} for P_{2a}–P_{2b} of 39% abated to 13% for P_{2a}–P_3 (Table 1), and the downward trend in P_3 was further highlighted by the mean RI_{i-j} for P_{2b}–P_3 becoming −23%. Standard errors of means remained quite constant over time (5–8%), but ranges (differences in most positive and negative values on an axis) varied between ~210% (RI_{1-2a} and RI_{2b-3}) and ~250% (RI_{2a-3}), from a halving to more than a doubling in species' responses. Nevertheless, the means of RI_{i-j} showed an overall "decrease–increase–decrease" oscillating behavior from P_1–P_{2a} to P_{2a}–P_{2b} to P_{2b}–P_3 (Table 1).

Across periods, mean values of mRI_{i-j} were always lower than those based on all trees (RI_{i-j}) by ~5–15% (Table 1). The largest differences were for P_1 and the lowest for P_3. This mostly reflected whether recruits were part of tree populations considered. Mean values of qRI_{i-j}, by contrast, were generally higher than those of RI_{i-j} for qRI_{1-2a}, qRI_{1-2b}, and qRI_{1-3} (all positive) by ~5–20%, but similar and slightly lower (more negative) by ~5–10% for qRI_{2a-2b}, qRI_{2a-3}, and qRI_{2b-3} (Table 1). This suggests that the faster-growing trees gained disproportionally more growth in P_3 compared with P_1 than did the slower-growing ones.

Relatively few species had pronounced responses. RI_{i-j} was significant ($P \le 0.01$) with two or more fold differences (i.e., $RI_{i-j} \ge 100\%$) for only eight of the 48 species, notably for *Dehaasia gigantocarpa*, *Dimorphocalyx muricatus*, and *Mallotus wrayi*. Patterns for these three species differed, although both *D. muricatus* and *M. wrayi* had positive values of RI_{1-2b}, RI_{1-3}, and RI_{2a-2b} (Table 1). The high variation in the patterns of

rgr over time—the basis to the changing RI_{i-j} values—is very apparent from the bar charts in Appendix S2: Fig. S1a–c.

Variation in RI_{i-j} within species was also very considerable. Although the range in mean species' RI_{i-j}, from the most negative to the most positive, was considerable (approximately −50 [−100] to 100 [150]%), the confidence limits themselves were almost as large (±50% to ±100%), so that even those species placed at the extremes of the ranges of species' RI_{i-j} values had moderately overlapping limits (Fig. 2). This suggests that changes from period to period in terms of rgr in stem size were extremely variable among individual trees. At the very most, for RI_{1-3} and RI_{2a-3}, 10–12 species revealed some non-overlapping limits which might indicate them to have been different from other species in their dynamics (Fig. 2c, e).

Dynamic inter-relationships

Two sets of Y-vs.-X diagrams were constructed: (1) "consecutive," where RI_{i-j} values were pairs of
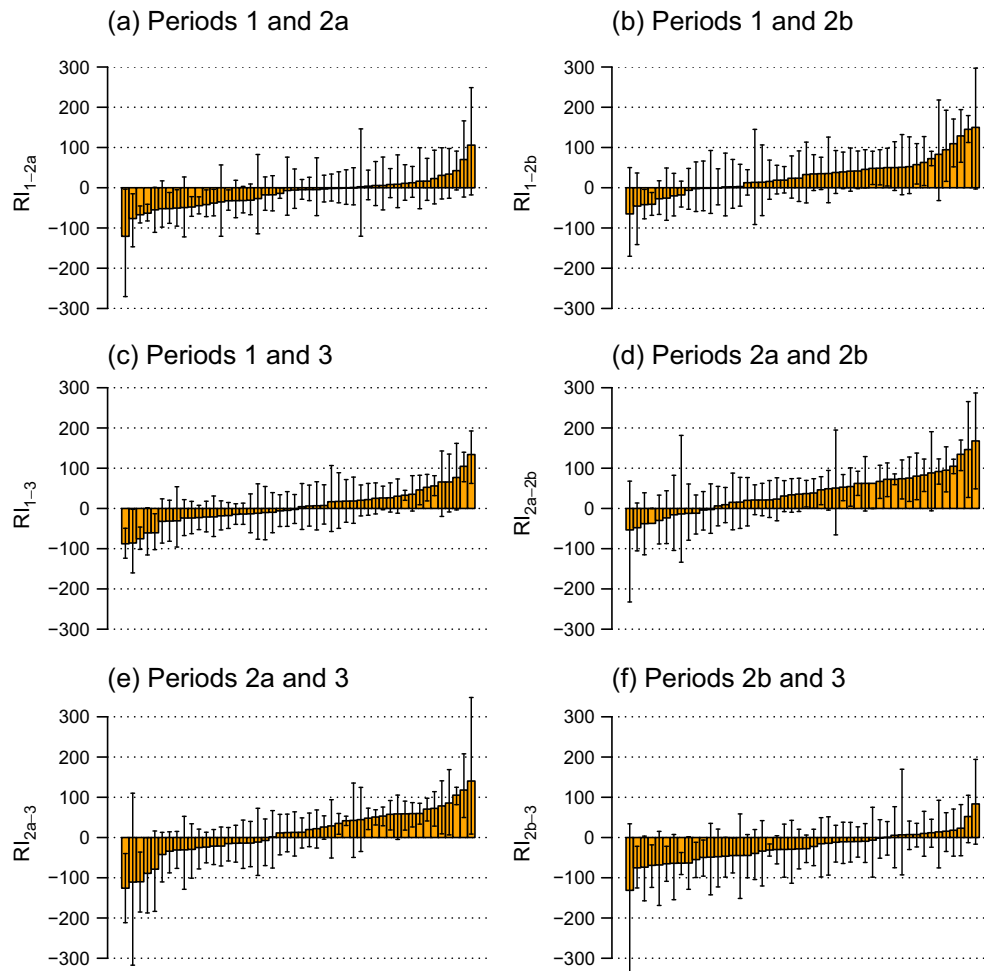

Fig. 2. Mean response indices (RI_{i-j}, %) in terms of period-weighted relative changes in stem relative growth rate for the 48 most abundant species as small trees (12.5 to <50 cm gbh) at Danum, ranked from highest to lowest, for the six pairwise indices possible across the four census periods (*i*–*j*): (a) P_1–P_{2a}, (b) P_1–P_{2b}, (c) P_1–P_3, (d) P_{2a}–P_{2b}, (e) P_{2a}–P_3, and (f) P_{2b}–P_3. The error bars are 95% confidence limits obtained, like the means, using a bootstrapping procedure. Species' codes are explained in Table 1. In (d), two species (*Hydnocarpus borneensis* and *Reinwardtiodendron humile*) lack limits because the standard errors found from procedure were exceptionally and unrealistically high.

periods following one another—period i of the y-axis was the same as period j of the x-axis after it: viz. P_{2a}–P_{2b} [$RI_{2a–2b}$] vs. P_1–P_{2a} [$RI_{1–2a}$] and P_{2b}–P_3 [$RI_{2b–3}$] vs. P_{2a}–P_{2b} [$RI_{2a–2b}$]—or by bridging one period viz. P_{2b}–P_3 [$RI_{2b–3}$] vs. P_1–P_{2b} [$RI_{1–2b}$] and P_{2a}–P_3 [$RI_{2a–3}$] vs. P_1–P_{2a} [$RI_{1–2a}$] (Fig. 3), and (2) "constitutive," where pairs of $RI_{i–j}$ had a period i in common, the y-axis $RI_{i–j}$ having a higher period j than the x-axis, viz. for P_1–P_{2b} [$RI_{1–2b}$] vs. P_1–P_{2a} [$RI_{1–2a}$], P_1–P_3 [$RI_{1–3}$] vs. P_1–P_{2a} [$RI_{1–2a}$], P_1–P_3 [$RI_{1–3}$] vs. P_1–P_{2b} [$RI_{1–2b}$], P_{2a}–P_3

[$RI_{2a–3}$] vs. P_{2a}–P_{2b} [$RI_{2a–2b}$] (Fig. 4). These eight combinations are all projecting forward in time (see Appendix S1: Table S3). Of the remaining seven of the 15 combinations possible in total, six would be projecting backward (period j the same on y- and x-axes) and the last is a uniquely dissociated pair (P_1–P_{2a} [$RI_{1–2a}$] vs. P_{2b}–P_3 [$RI_{2b–3}$]). These last mentioned pairs would neither follow the "arrow of time" nor share a common period, and so they are not considered further in the analysis of this paper. Consecutive diagrams allow an
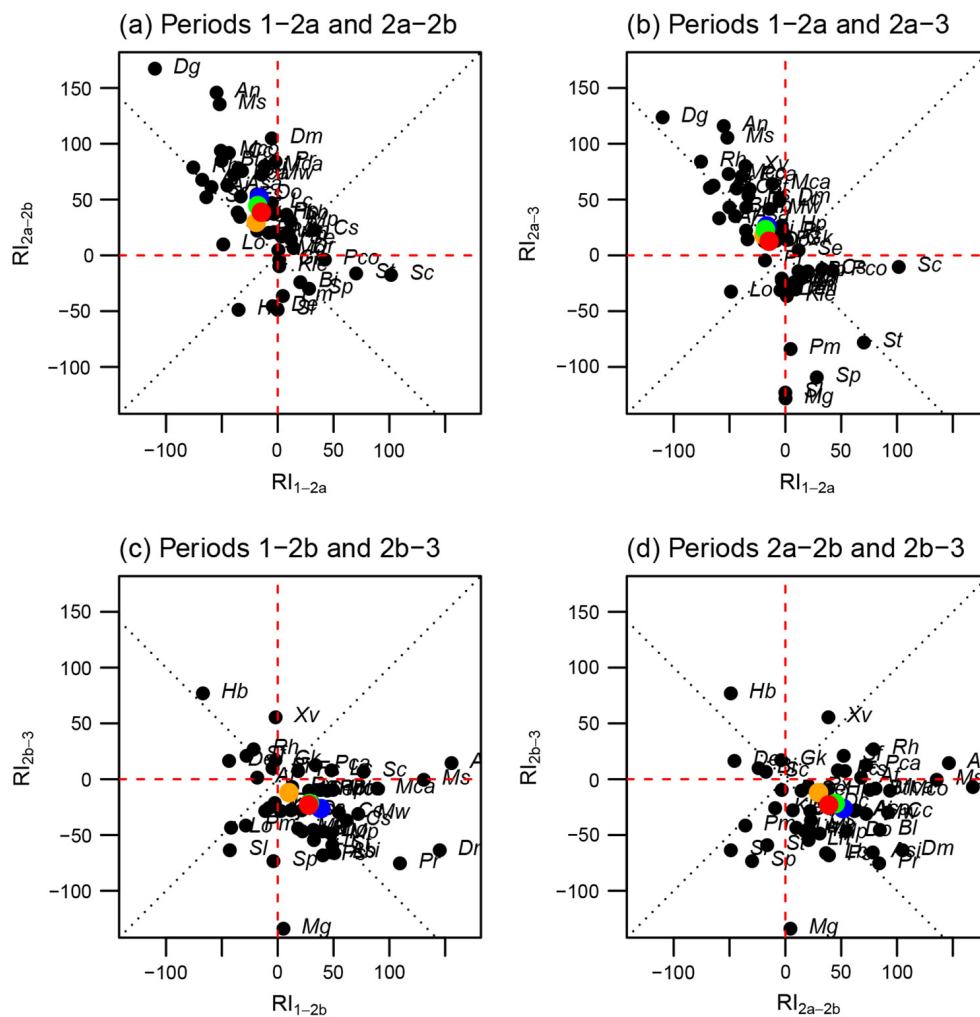

Fig. 3. Pairs of response indices ($RI_{i–j}$, %), in terms of stem relative growth rates of the 48 most abundant species as small trees (12.5 to <50 cm gbh) at Danum, plotted against one another (i–j progression diagrams) for cases in which two periods were "consecutive": (a) $P_{2a–2b}$ vs. $P_{1–2a}$, (b) $P_{2a–3}$ vs. $P_{1–2a}$, (c) $P_{2b–3}$ vs. $P_{1–2b}$, and (d) $P_{2b–3}$ vs. $P_{2a–2b}$. Species' codes are explained in Table 1. Dashed red lines define the quadrants for ±change in $RI_{i–j}$ values. Colored point coding: mean $RI_{i–j}$ of all trees of the 48 species together (blue), of all other species besides the 48 (orange), all species' trees in the plots (green), and the mean of the 48 species' $RI_{i–j}$ means (red).
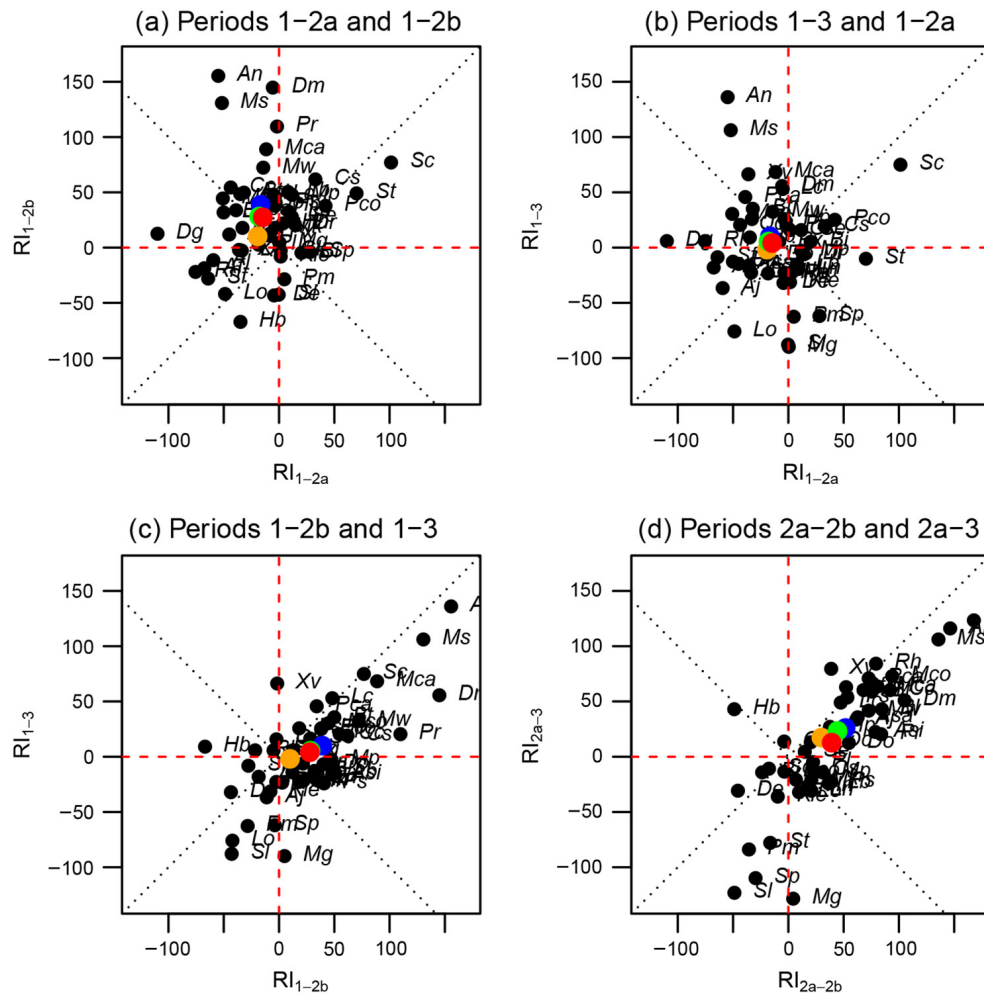
Fig. 4. Pairs of response indices ($RI_{i–j}$, %), in terms of stem relative growth rates of the 48 most abundant species as small trees (12.5 to <50 cm gbh) at Danum, plotted against one another ($i–j$ stability diagrams) for cases which were "constitutive": (a) $P_{1–2b}$ vs. $P_{1–2a}$, (b) $P_{1–3}$ vs. $P_{1–2a}$, (c) $P_{1–3}$ vs. $P_{1–2b}$, and (d) $P_{2a–3}$ vs. $P_{2a–2b}$. Species' codes are explained in Table 1. Dashed red lines define the quadrants for ±change in $RI_{i–j}$ values. Colored point coding as in Fig. 3.

assessment of progression in, or continuation of, dynamics with time, and constitutive diagrams allow an assessment of stability in, or reflection of, the dynamics. They complement one another.

Of the consecutive cases, and where P_{2a} was pivotal, $RI_{1–2a}$ and $RI_{2a–2b}$ were strongly negatively correlated ($r = -0.657$, $P < 0.001$; Fig. 3a), and likewise so were $RI_{1–2a}$ and $RI_{2a–3}$ ($r = -0.604$, $P < 0.001$; Fig. 3b). However, where P_{2a} was not pivotal, the correlations were all but lost: for $RI_{1–2b}$ and $RI_{2b–3}$ ($r = -0.200$, $P = 0.17$; Fig. 3c) and for $RI_{2a–2b}$ and $RI_{2b–3}$ ($r = 0.053$, $P = 0.72$; Fig. 3d). Most species lie in the negative $RI_{1–2a}$/positive

$RI_{2a–2b}$ or $RI_{2a–3}$ and positive $RI_{1–2a}$/negative $RI_{2a–2b}$ or $RI_{2a–3}$ quadrants of Fig. 3a, b, with relatively more in that upper left one in Fig. 3a than in b. Very differently, a majority of species lie in the positive $RI_{1–2b}$ or $RI_{2a–2b}$ /negative $RI_{2b–3}$ quadrant in Fig. 3c, d, and relatively few for both in the opposite, upper right, one.

Of the constitutive cases, $RI_{1–2a}$ showed a weakly positive non-significant correlation with $RI_{1–2b}$ ($r = 0.150$, df = 46, $P = 0.31$), and a full range of combined responses (Fig. 4a) with predominantly negative values for $RI_{1–2a}$ and predominantly positive ones for $RI_{1–2b}$. The least

frequently occupied quadrant was the positive RI_{1-2a}/negative RI_{1-2b}. For RI_{1-3} vs. RI_{1-2a} ($r = -0.061$, $P = 0.68$; Fig. 4b), the proportion of negative values increased to about one half, indicating a stabilizing effect in P_3. In contrast, RI_{1-2b} and RI_{1-3} were more significantly positively correlated ($r = 0.712$, $P < 0.001$), the quadrant of negative RI_{1-2b}/positive RI_{1-3} being very much the minority (Fig. 4c). Thus, the growth changes from P_1 to P_{2a} and P_1 to P_{2b} showed most variation among species, but those of P_{2b} tended to continue into P_3. These periods form the basis of the three key stability graphs. RI_{2a-2b} and RI_{2a-3} were even more strongly correlated ($r = 0.800$, $P < 0.001$; Fig. 4d). Correlations for these stability diagrams are only indicative of trends among indices as i and j change because, in the constitutive cases at least, they share the rgr values of one period, and so their variables would not be fully independent (but see randomization tests later to overcome this problem).

Interpreting the RI graphs

The first two consecutive RI_{i-j}-vs.-RI_{i-j} graphs allowed an analysis of *fundamental progression* where either the change from P_{2a} to P_{2b} alone (RI_{2a-2b}, post-reaction 1 phase; Fig. 3a) or the change from P_{2a} to P_3 (RI_{2a-3}, post-reaction 1 and 2 phases; Fig. 3b) was plotted against the change from P_1 to P_{2a} (RI_{1-2a}, the reaction phase). The remaining two graphs indicate *implicit* and *explicit progression*, where the later change from P_{2b} to P_3 (RI_{2b-3}, post-reaction 2 phase) was plotted against either the change from P_1 to P_{2b}, P_{2a} being implicit in having a latent effect (RI_{1-2b}, reaction and post-reaction 1; Fig. 3c) or against the change from P_{2a} to P_{2b} (RI_{2a-2b}, post-reaction 1 phase alone; Fig. 3d), P_{2a} being now at the start and therefore explicit.

The first two constitutive RI_{i-j}-vs.-RI_{i-j} graphs allowed for an analysis of *fundamental stability* because they plot response from P_1, before the P_{2a} perturbation, to after it in either P_{2b} or P_3 (RI_{1-2b} and RI_{1-3}, including the reaction and either one or both of post-reaction phases 1 and 2) vs. the response from P_1 to that period P_{2a} with the perturbation (RI_{1-2a}, the reaction phase; Fig. 4a, b). Where responses were over a longer time, that is, from P_1 to P_3 (RI_{1-3}), and this was plotted against a period including P_{2a} (RI_{1-2b}, reaction and post-reaction 1 phases), an analysis

of *intended stability* was permitted (Fig. 4c). The fourth constitutive graph, plotting the period with both post-reaction 1 and 2 phases (RI_{2a-3}) vs. post-reaction 1 (RI_{2a-2b}) allowed an analysis of *extended stability* (Fig. 4d) since P_{2a} was the starting period. Stability analysis requires a common period at the start of the changes, one to which later changes in rgr may or may not have returned, even though it can incur a degree of carried-over interdependence.

Simulation of RI.—A simple simulation allows an understanding of stability from the constitutive diagrams. The eight cases in Fig. 5a lead to the eight labeled points in Fig. 5b, one per octant. Although shown for RI_{1-2b} vs. RI_{1-2a}, they equally apply in their interpretation to RI_{1-3} vs. RI_{1-2a} and RI_{1-3} vs. RI_{1-2b}, in the latter case with no knowledge of P_{2a} involved. The four upper panels in Fig. 5a have stable outcomes: With or without a part oscillation, rgr in P_{2b} is closer to that in P_1 than in P_{2a}. This first set results in the condition $|RI_{1-2a}| > |RI_{1-2b}|$, represented by the left and right middle pairs of octants in Fig. 5b. The lower four panels of Fig. 5a have unstable outcomes: With or without a part oscillation again, rgr in P_{2b} is further from that in P_1 than in P_{2a}. This second set results in the condition $|RI_{1-2a}| < |RI_{1-2b}|$, represented by top and bottom middle pairs of octants in Fig. 5b. Although the RI_{i-j} values in Fig. 5b are shown symmetrically placed, the rgr values leading to them do not have exactly similar positive and negative progressions (Fig. 5a). Had the latter been the case, a slight asymmetry would arise because of the period length weightings applied in the formula for RI_{i-j} (see also Appendix S1: Fig. S1).

Using this system, species can be differentiated into those showing stable, as opposed to unstable, growth responses, irrespective of any small shifts within quadrants due to weighting. A species that indicates stability by P_{2b} is more resilient than one that shows it by P_3. Although a similar interpretation can be applied to the consecutive diagrams, the octants do not align with the eight cases properly, showing on the left and right halves of Fig. 5c, respectively, upward and downward vertical displacements. The lack of a common originating period means that stable and unstable oscillations are not readily distinguishable from one another in a diagnostic manner in the consecutive case.
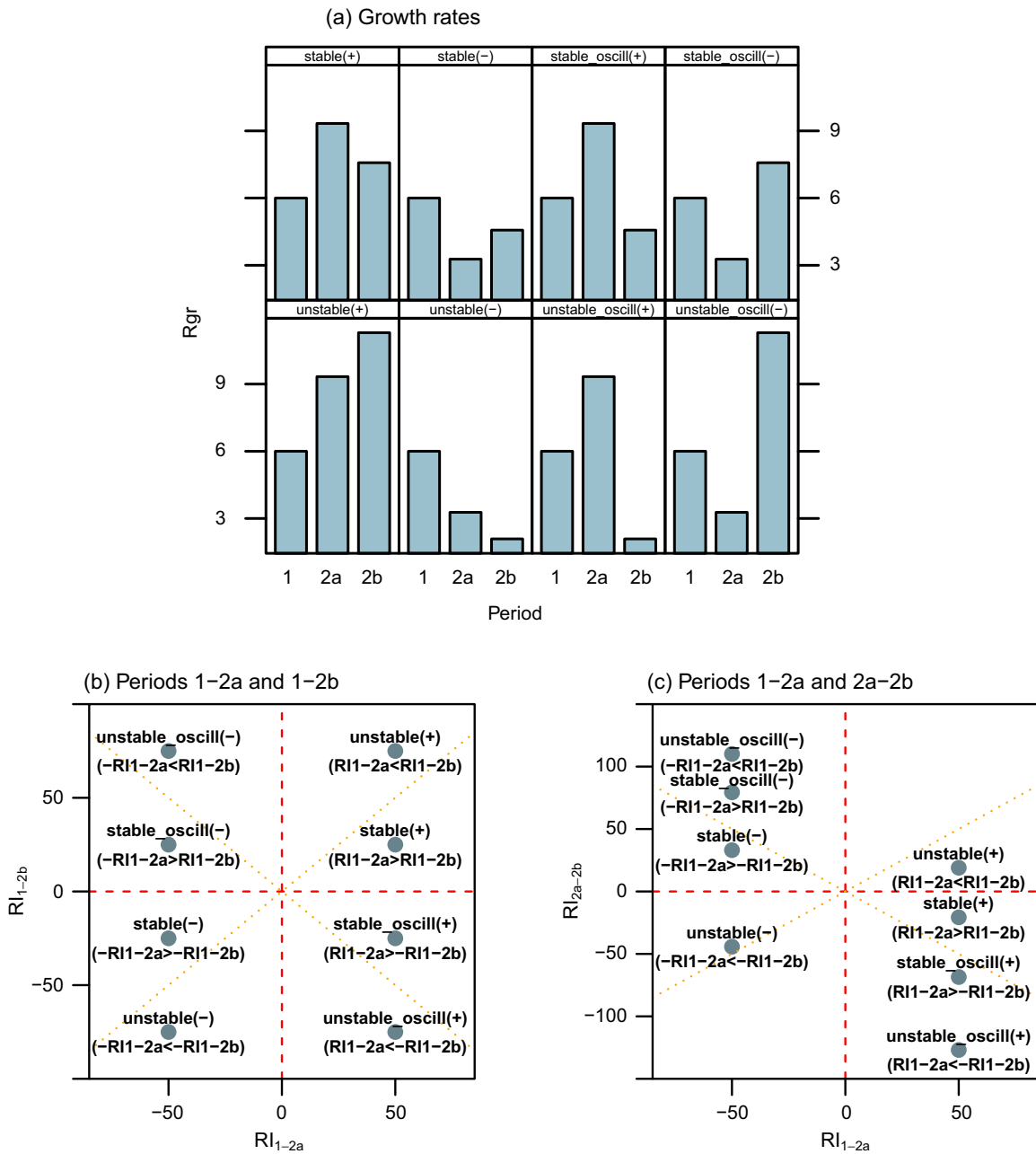
Fig. 5. Interpretation of paired response index (RI_{i-j}, %) diagrams, using (a) eight constructed sets of rgr values over three periods (P_1–P_3) to illustrate the resulting stabilizing and oscillatory dynamics in primarily the (b) constitutive (stability) case, but also how that becomes reflected in (c) the related consecutive (progression) case.

Progression

Those species whose growth change in the post-reaction 1 phase (RI_{2a-2b}) was in the opposite direction to that in the reaction phase (RI_{1-2a})—negative reaction became positive post-reaction (and vice versa)—were interpreted as showing compensation, while those that continued growth changes in the same direction as in the reaction phase showed decompensation, each being classified by the direction (or sign) of the reaction. Hence, in the upper left quadrant of Fig. 3a are 29 species (60.4% of the 48, Table 2a;

Table 2. Species at Danum showing (a) progression and (b) stabilization in their relative growth rates affected by drought perturbation, from two analyses using different indices, early (RI_{1-2b}, RI_{2a-2b}) and late (RI_{1-3}, RI_{2a-3}, respectively) after the event, graphed against (RI_{1-2a}), while meeting the condition of $RI_{ij} > |20\%|$ for at least one of the pairs of values, and where reaction to the perturbation (response) was either positive (+) or negative (−), so that in (a) the species listed are those compensating (i.e., growth change opposite to the reaction) and in (b) the form of stability was either returning (R) or oscillating (O; see text).

Analysis	Response	Stability	Species codes	Mean OUI (range)
(a) Progression				
1. RI_{1-2a} vs. RI_{2a-2b}	+		Bi, Pm, Pco, Sc, Sp, St	46 (18–66)
	−		Af, Aj, An, Asa, Asi, Bl, Bt, Cc, Dc, Dg, Dm, Do, Fs, Hp, Lc, Lo#, Mca, Mco, Mk#, Ms, Mw, Pca, Pl#, Pr, Ps#, Px#, Rh, Sf, Xv	25 (0–63)
2. RI_{1-2a} vs. RI_{2a-3}	+		Bi, Cs, Dr, Hn, Kle, Lb, Ln, Mg, Pco, Pm, Sc, Sp, St	36 (6–66)
	−		Af, Aj, An, Asa, Asi, Bl, Bt, Cc, Dc, Dg, Dm, Do, Fs, Hn##, Hp, Lc, Mca, Mco, Ms, Mw, Pca, Pr, Rh, Sf, Xv	23 (0–60)
(b) Stabilization				
1. RI_{1-2a} vs. RI_{1-2b}	+	R	Pco, Sc, St	42 (30–58)
		O	Bi, Sp	42 (18–66)
	−	R	Asa, Bl, Dg, Fs, Mco, Pca	17 (1–60)
		O	Af, Aj, Dc, Lo, Rh, Sf, Xr	35 (18–54)
2. RI_{1-2b} vs. RI_{1-3}	+	R	Bi, Cs*, Pco, Sc	34 (18–49)
		O	St	57 (–)
	−	R	Af, Aj, Asa, Asi*, Bl, Dc, Sf	39 (7–60)
		O	Cc*, Dg, Fs*, Hb*, Mco, Rh	9 (1–18)

Notes: OUI, over–understory index (see main text). Codes for species are found in Table 1. In (a), the species with a "#" superscript compensated by P_{2b} but lost it by P_3 and that with a "##" only gained it first by P_3, and in (b), the asterisked species found by analysis 2 are those of relatively lower resilience compared with all of the species found by analysis 1.

$RI_{i-j} \geq 20\%$ for at least one of the pair of axes) showing compensation after a negative RI_{1-2a}, and in the lower right quadrant of the same figure just six species (12.5%, Table 2a) showing the opposite result. Decompensation was much less frequent than compensation.

In a similar approach, when the post-reaction was for the 1 and 2 phases (RI_{1-3}), there were slightly fewer species showing negative compensation (25/48 or 52.1%, Table 2a, $RI_{i-j} \geq 20\%$ as before) but relatively more with positive compensation (13/48 or 27.1%, Table 2a), and again relatively few showing decompensation (Fig. 3b). Of the 29 species showing progression in the shorter post-reaction 1 phase, 24 also showed it in post-reaction phase 2 (Table 2a). Further, 24/25 species with negative compensation in this progression were among those with the same compensation for the shorter post-reaction period (Fig. 3a). Conversely, all six of the species with positive compensation in the shorter period were among those for the longer post-reaction period (Table 2a).

For the intended progression, a large proportion of the species (26/48, 54.2%; $RI_{i-j} \geq 20\%$) showed positive compensation in the lower right quadrant (Fig. 3c), that is, after achieving positive RI_{1-2b} (P_{2a} within, reaction plus post-reaction 1 phases), since these species reversed their growth rate direction in P_{2b} to P_3 (RI_{2b-3}). When this "settling-down" effect was plotted against the post-reaction phase 1 only (RI_{2a-2b}), the extended progression, the result was confirmed (28/48 species or 58.3%). Interestingly, the three species placed more extremely remained the same in both cases. Furthermore, 16/26 species and 21/28 species, with positive compensation in Fig. 3c, d, respectively, are among those species showing negative compensation in Fig. 3a, indicating later re-compensation of earlier compensation by about half the species affected.

The permutation tests indicated that the all species' consecutive relationships between RI_{1-2a} and RI_{2a-2b}, and RI_{1-2a} and RI_{2a-3} were significantly more negatively steep than expected under the null model (Table 3a), and this was even stronger in effect among just the understory species (Table 3b). Therefore, some species were responding more strongly than others, moving the slope of the line from ~−1.0 toward −1.3 to −1.8, that is,

Table 3. Standardized major-axis (SMA) regression statistics for the relationships between pairs of response indices (RI$_{i–j}$), where the first of the pair is plotted on the x-axis and the second on the y-axis for consecutive (Fig. 3) and constitutive (Fig. 4) combinations: (a) all 48, and (b) the 17 understory, species.

Species set and graph type	RI for periods	Observed		Expected	
		a	b	b	P
(a) All species					
Consecutive	1, 2a vs. 2a, 2b	19.3	−1.33	−0.92	***
	1, 2a vs. 2a, 3	−9.8	−1.54	−0.90	***
	1, 2b vs. 2b, 3	−1.0	−0.79	−0.84	ns
	2a, 2b vs. 2b, 3	−51.6	0.75	−0.99	***
Constitutive	1, 2a vs. 1, 2b	45.8	1.26	1.10	ns
	1, 2a vs. 1, 3	−13.6	−1.20	0.83	***
	1, 2b vs. 1, 3	−22.2	0.95	0.76	*
	2a, 2b vs. 2a, 3	−32.2	1.16	0.98	†
(b) Understory species					
Consecutive	1, 2a vs. 2a, 2b	7.6	−1.79	−1.02	***
	1, 2a vs. 2a, 3	−17.0	−1.84	−0.98	***
	1, 2b vs. 2b, 3	10.3	−0.77	−0.89	ns
	2a, 2b vs. 2b, 3	25.7	−0.75	−1.00	ns
Constitutive	1, 2a vs. 1, 2b	84.8	1.74	1.13	†
	1, 2a vs. 1, 3	−26.7	−1.52	0.89	***
	1, 2b vs. 1, 3	−15.5	0.87	0.78	ns
	2a, 2b vs. 2a, 3	−24.8	1.03	0.98	ns

Note: Randomized permutation tests gave expected mean slopes and confidence limits.
*** $P \leq 0.01$; * $P \leq 0.05$; † $P \leq 0.10$; ns, $P > 0.10$

from stable toward unstable oscillatory response (refer to Fig. 5c). None of the slopes (b-values) for intermediate and overstory species, taken independently as groups, was significant ($P > 0.1$). Referring to those species also with highly significant changes in RI$_{i–j}$ in Table 1, the understory species being apparently most strongly *destabilized* were *D. gigantocarpa*, *D. muricatus*, *Antidesma neurocarpum*, and *Magnolia gigantifolia* (Fig. 6a, b).

Stability

The analysis using RI$_{1–2b}$ vs. RI$_{1–2a}$ (Fig. 4a) indicated just nine species (three with an initially positive response to the perturbation and six with a negative one) having returning stability and nine others (two and seven responding positively and negatively initially, respectively) having oscillatory stability, 19/48 or 39.6% of the species (Table 2b). The comparable analysis using RI$_{1–3}$ vs. RI$_{1–2a}$ (Fig. 4b) indicated three more species with returning, and one more with oscillatory, stability, thus resulting in 22/48 species (45.8%) stabilizing (Table 2b). Twelve of the 18 species with some form of stability from the first analysis showed that it also from the second analysis. Thus, a majority of species (26/48,

54.2%) indicated lack of stability. All 18 species in that first analysis were, by definition, more resilient (i.e., stabilizing first or latest by P$_{2b}$) than the remaining seven (i.e., doing so by P$_3$), as indicated in Table 2b. Given this agreement between the stability analyses, and together with the remaining species showing instability in roughly similar ways, the positive trend in Fig. 4c is to be then expected, with a tight cluster of 12 species behaving very similarly across periods (third octant) and most species lying below the positively inclined diagonal (38/48, RI$_{1–3}$ < RI$_{1–2b}$). Recovery of species after the perturbation was seen to generally continue or be emphasized by the even tighter relationship in Fig. 4d (RI$_{2a–3}$ < RI$_{2a–2b}$), indicating further that between the perturbation-free periods P$_{2b}$ and P$_3$ not so much of importance was happening in terms of growth dynamics. Coding species with stable rgr dynamics as "1" and those unstable with "0," logistic regressions of stability on the logarithm of mean population size (across the censuses studied) showed no statistical significance ($P = 0.96$ and 0.85, respectively, for RI$_{1–2b}$ vs. RI$_{1–2a}$ and RI$_{1–3}$ vs. <RI$_{1–2a}$). This means that species' stabilities were unrelated to rareness or commonness.
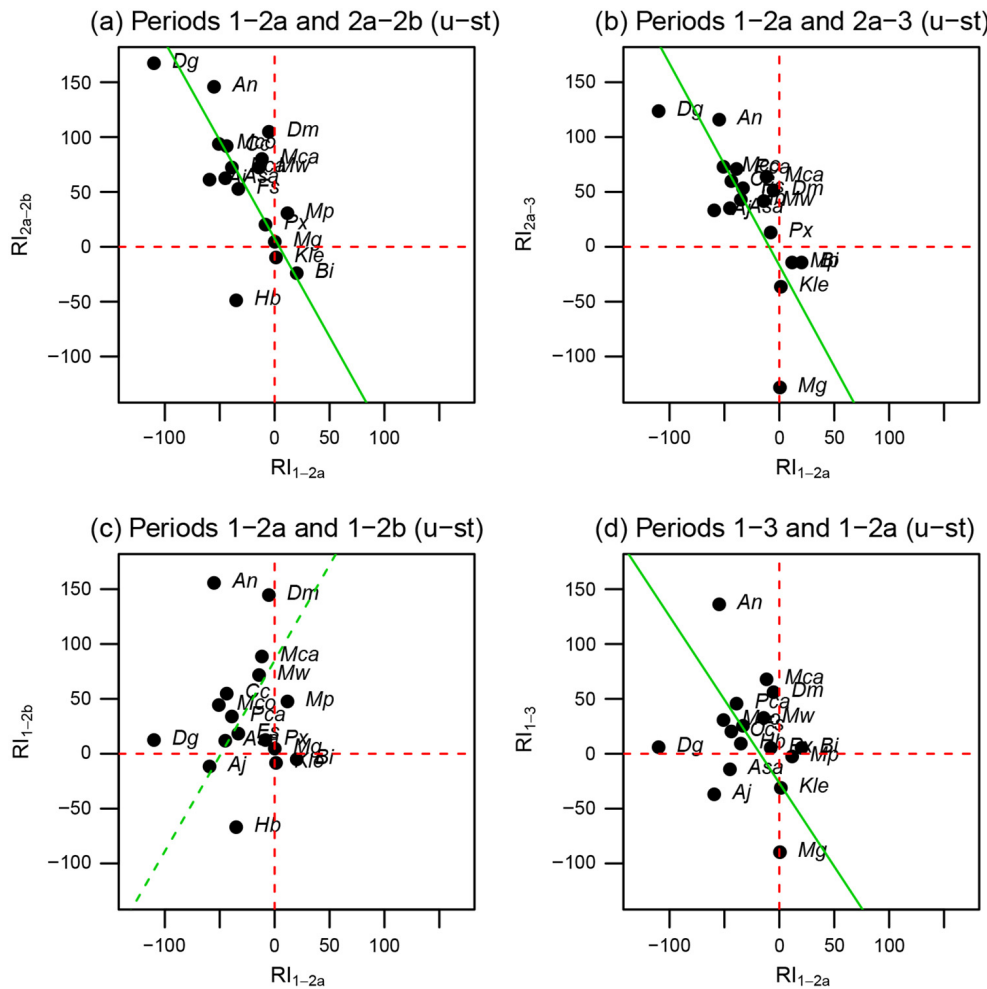
Fig. 6. Pairs of response indices (RI$_{i-j}$, %), in terms of stem relative growth rates of the 17 understory species as small trees (12.5 to <50 cm gbh) at Danum, plotted against one another (*i–j* progression and stability diagrams) for cases which were "consecutive" (a) P$_{2a-2b}$ vs. P$_{1-2a}$ (b) P$_{2a-3}$ vs. P$_{1-2a}$, or "constitutive" (c) P$_{1-2b}$ vs. P$_{1-2a}$ and (d) P$_{1-3}$ vs. P$_{1-2a}$. Species' codes are explained in Table 1. The full green lines are the model regression fits (see text) at *P* < 0.001, while the dashed line (in c) is marginally significant at *P* < 0.10.

The permutation tests here indicated that just the constitutive all species' relationship between RI$_{1-2a}$ and RI$_{1-3}$ (and rather surprisingly not RI$_{1-2a}$ and RI$_{1-2b}$) was significant compared with the null model, indicating a strong and delayed shift from stable to unstable oscillations among some species (refer to Fig. 5b), again also a stronger effect being found when understory species were considered alone. As with progression, intermediate and overstory species showed no significant relationships when taken as independent groups (*P* > 0.1): The understory species

apparently most *destabilized* were *A. neuro-carpum*, *D. muricatus*, *Magnolia candollei*, and *M. gigantifolia* (Fig. 6c, d). The seven most abundant species in the understory with *n* ≥ 50 individuals on average across censuses illustrate the varying dynamics well (Fig. 7). The ordered starting set of RI$_{1-2a}$ values are replaced by more disarranged values for RI$_{1-2b}$ and RI$_{1-3}$, and likewise for RI$_{2a-2b}$ and RI$_{2a-3}$, to show—with the exception of *Fordia splendidissima* and *Polyalthia cauliflora*—a generally inverse pattern to RI$_{1-2a}$ for RI$_{2b-3}$.
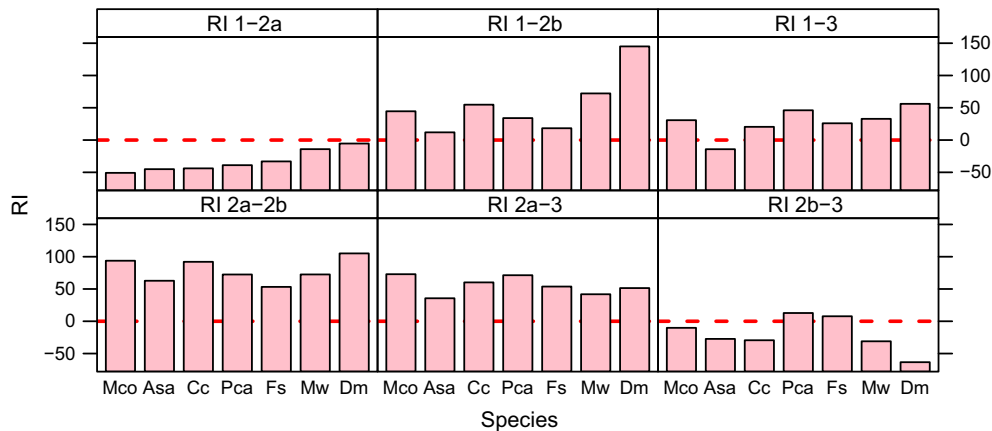
Fig. 7. Change in mean response indices (RI_{i-j}, %) in terms of stem relative growth rates of the seven most abundant understory species ($n \geq 50$ trees) across successive periods, ranked according to the initial responses in P_1–P_{2a}. Species' codes are explained in Table 1.

Change to mRI and qRI

Correlations between all RI_{i-j} variables, as ordered across the columns in Table 1, and those based on matched-tree, rgr_m, mRI_{i-j} were high ($r = 0.769$, 0.861, 0.830, 0.933, 0.944, and 0.914; $n = 48$, all $P < 0.001$). Perhaps only in the first three cases (RI_{1-2a} to RI_{1-3}) do major differences occur: The outliers were, respectively, *M. gigantifolia* and *Syzygium tawaense*, *Syzygium elopurae* and *Diospyros elliptifolia*, *Hydnocarpus borneensis* and *Shorea fallax* (the first of each pair having $rgr_m > rgr_{all}$, the second the converse). Hence, ignoring recruits in the second period and deaths after the first one had rather little effect on the RI_{i-j} values apart from the very few exceptions mentioned.

Do the qRI_{i-j} values explain differences between species better? Correlations between these and all-species RI_{i-j} values ($n = 48$) were also high ($r = 0.753$, 0.921, 0.938, 0.799, 0.920, and 0.872). In the graphs where RI_{i-j} values involved rgr in P_{2a}, the three species *A. neurocarpum*, *Reinwardtiodendron humile*, and *D. gigantocarpa* were outlying, their rgr_q values $\gg$ the rgr_{all} ones for RI_{1-2a}, but the opposite for RI_{2a-2b} and RI_{2a-3}. The unusual distributions of species' rgr values, in P_{2a} especially, were also noted in Newbery et al. (2011).

Response in relation to story

The relationships between RI_{i-j} and OUI revealed several significant and interesting patterns for the 48 species (Fig. 8). For RI_{i-j} changes between P_1 and P_{2a}, the correlation with OUI was positive but marginally non-significant ($r = 0.272$, df = 46, $P = 0.061$), with species spread close to, yet mostly just below, the $RI_{i-j} = 0$ line. Between P_1 and P_{2b}, although the changes were generally positive, RI_{i-j} declined more steeply ($r = -0.289$, $P = 0.022$), with much higher values for species with low OUI values (true understory species) than those with high ones (overstory species), the line pivoting around $RI_{i-j} = 0$ at OUI ~60%. This negatively inclined line shifted downward and the correlation became even more significant for P_1–P_3 ($r = -0.424$, $P = 0.003$), with the understory species maintaining a relatively high positive RI_{i-j} and the overstory ones now having negative RI_{i-j} values. The P_{2a}-to-P_{2b} [RI_{2a-2b}] and P_{2a}-to-P_3 [RI_{2a-3}] relationships ($r = -0.397$, $P = 0.005$; and $r = -0.462$, $P = 0.001$, respectively) are similar to those mentioned for P_1-to-P_{2b} and P_1-to-P_3 relationship. Finally, RI_{2b-3}, for P_{2b}-to-P_3 relationship, was not significantly correlated with OUI ($r = -0.228$, $P = 0.12$)—although with largely slightly negative RI_{i-j} values indicating a dying away of the response between these two periods.

The way in which the fitted lines rise, change direction of slope, and finally settle in Fig. 8 (panel sequence "a-b-d-f" or "a-d-e-f") suggests that the stabilizing process was being mediated by structural guild (story as in the OUI). On none of the eight RI_{i-j}-vs.-RI_{i-j} graphs in Figs. 3 and 4 could OUI groups be statistically discriminated from one another, though. Only 43–55% of the 48
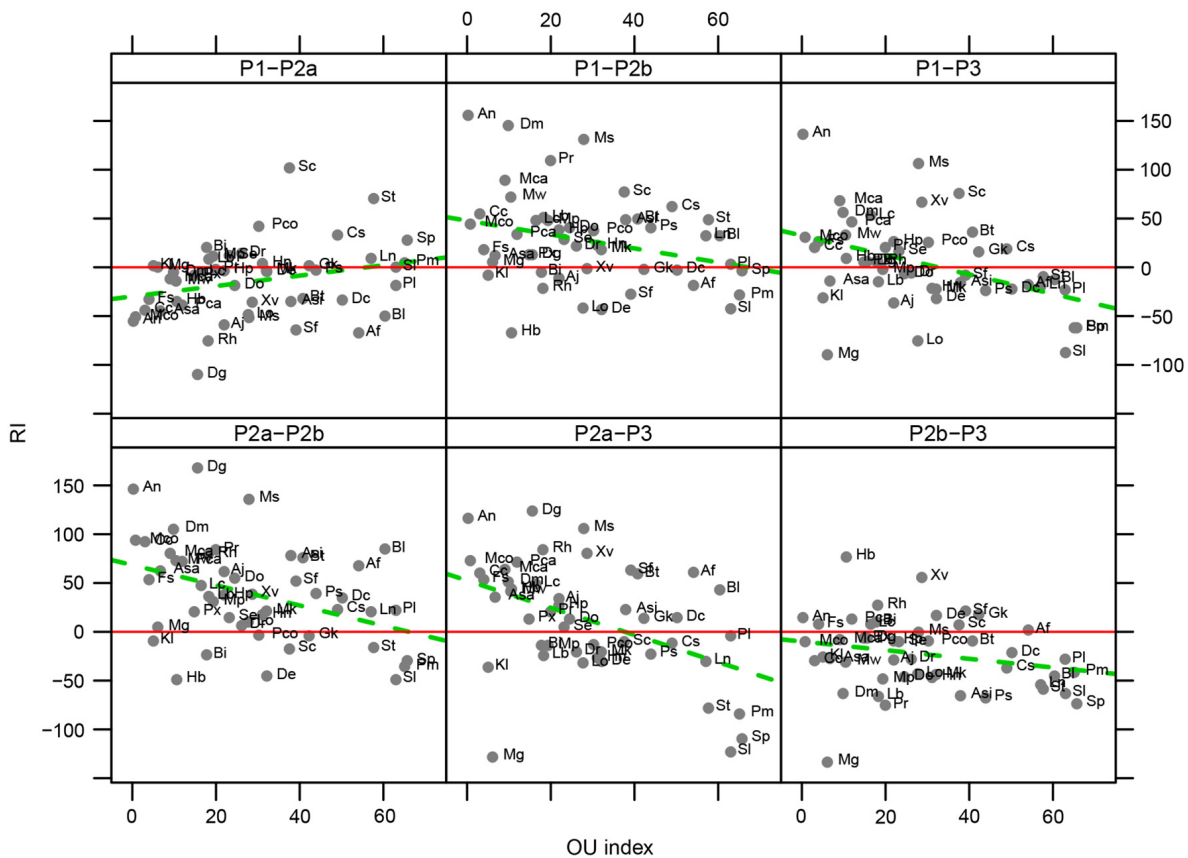
Fig. 8. Mean response indices (RI_{i-j}, %) in terms of stem relative growth rates of the 48 most abundant species as small trees (12.5 to <50 cm gbh) at Danum plotted against their over–understory index (OUI; based on trees ≥10 cm gbh—see text), for the six $i–j$ period combinations (panels): $P_1–P_{2a}$, $P_1–P_{2b}$, $P_1–P_3$, $P_{2a}–P_{2b}$, $P_{2a}–P_3$, and $P_{2b}–P_3$. The green dashed lines are simple linear regression fits to illustrate trends; red lines represent zero change between periods. Species' codes are explained in Table 1.

species were correctly allocated to their stories, giving little support to the idea that some OUI groups per se (i.e., in their entirety) were perhaps more stable than others. Among the species characterizing the quadrants for the two first progression graphs (consecutive periods), no strong differences in OUI values were apparent (Table 2a), except that positive responses for RI_{1-2a} vs. RI_{2a-2b} involved no understory species (OUI < 18). For the octants of the two first stability graphs (constitutive periods), returning responses had notably low means and ranges of OUI values for RI_{1-2a} vs. RI_{1-2b} excluding overstory species, and likewise low values for oscillating negative responses for RI_{1-2a} vs. RI_{1-3} (Table 2b).

Trends in the qRI_{i-j} values based on rgr_q in relation to OUI were very similar to RI_{i-j} with rgr_{all},

but while correlations were weaker at the start and end of the panel sequence of Fig. 8, that is, between P_1 and P_{2a} (RI_{1-2a}; $r = 0.182$, df = 46, $P = 0.22$) and between P_{2b} and P_3 (RI_{2b-3}; $r = -0.229$, $P = 0.12$), they were as strong for the RI_{i-j} values of the periods in between (P_1-to-P_{2b} [RI_{1-2b}]: $r = -0.313$, $P = 0.031$; P_1-to-P_3 [RI_{1-3}]: $r = 0.430$, $P = 0.002$; P_{2a}-to-P_{2b} [RI_{2a-2b}]: $r = -0.412$, $P = 0.004$; and P_{2a}-to-P_3 [RI_{2a-3}]: $r = -0.497$, $P < 0.001$). The corresponding mRI_{i-j} vs. OUI diagrams (not shown) were similar to the RI_{i-j} ones: mRI_{1-2a} ($r = 0.145$, $P = 0.33$) and mRI_{2b-3} ($r = -0.173$, $P = 0.23$), with mRI_{1-2b}, RI_{1-3}, RI_{2a-2b}, and RI_{2a-3} ($r = -0.309$, $P = 0.032$; $r = -0.399$, $P = 0.005$; $r = -0.281$, $P = 0.053$; and $r = -0.396$, $P = 0.005$, respectively), indicating again little loss in robustness when RI_{i-j} adjusted

for the dynamics variables determining species' sample composition.

Discussion

Temporal and spatial complexity

The approach here is a simple form of multivariate or community time-series analysis. It used four periods of change across five censuses, resulting in four consecutive and four constitutive pairwise diagrams of RI_{i-j}. Had there been only three periods, the number of diagrams would have been only one of each kind from the three combinations possible. Nevertheless, to have had to deal with five periods would have resulted in an almost unmanageable level of temporal complexity with 10 consecutive and 10 constitutive diagrams out of the 45 combinations possible (Appendix S1: Table S3). In future considerations of the recent fifth main census (sixth for the subplots), a sliding window of four periods might still just be operational.

The changes over the three phases showed a very general basic oscillation of decrease, increase, and decrease in RI_{i-j}, with similar changes with mRI_{i-j} and qRI_{i-j} (Table 1). The species' averages (colored symbols in Figs. 3 and 4) show small changes and follow the same general pattern. The very large variation within-species responses led to considerable overlap of species' patterns. Large and small values of RI_{i-j} appear unrelated to species abundance. The pivotal role of P_{2a} provided essential evidence of the perturbation's effect (Fig. 1), shown by the change in correlations across periods and the shifts in position of the main cluster of species' points across quadrants in the RI_{i-j}-vs.-RI_{i-j} diagrams. Overall, the constitutive cases showed stability at the community level but with also some lag from P_{2b} to P_3. There is evidence of a fundamental progression in that responses are changing largely positively after the perturbation (post-reaction phases 1 and 2), although the data do not allow implicit and explicit progression to be differentiated. Many species tended to stabilize their growth dynamics but compared with intended stabilization, extended stabilization began to reveal some further unexpected variation, especially in the form of unstable oscillations by P_3. Stability and instability were unrelated to species abundance.

Once the constraining effects of the dry period had passed, some species showed new responses: The perturbation caused very complicated dynamics with a tendency to break away from stabilizing responses into more unstable oscillatory ones. The species with large RI_{i-j} values had strong influences on the slopes of the fitted SMA regression lines: The majority of species with smaller RI_{i-j} values near to the means and centers of the diagrams ($\{0, 0\}$) were being offset by these different species' strong responses. The majority of the species were acting as part of this general stabilization of rgr, but a notable portion were destabilizing it. This is rather analogous to the drift and diffusion in physical systems, the more responsive and destabilizing species leading to the increased variances (diffusion) over and above the main shift (drift). Such dynamics were undoubtedly also influenced by the earlier and recent smaller perturbations in 1987 and 1992, as well as the stronger one equivalent to 1998 occurring in 1983 (Newbery and Lingenfelder 2004, 2009). Perturbations as a representation of environmental stochasticity introduced important variability into the dynamics of the tree community at Danum.

Set against an overall oscillation in rgr with time, there was considerable between- and within-species variation in any one period. P_2 was again pivotal, having the most influence on relative changes in response. Many species (approximately a half) were affected in P_{2a}, positively or negatively and then stabilizing: Their growth temporarily enhanced or suppressed. The general pattern continued into P_3, with many species continuing to stabilize or experience oscillations.

The various dynamics of the different species at Danum with respect to growth are complicated because, aside from a large degree of species specificity (Newbery et al. 1999) defined by characteristically average rates, growth will be determined by tree size, its neighborhood affecting competition, and growth histories of the individuals. By focusing on a key size class—the small understory trees—we isolated the grosser size effects on rgr (Newbery et al. 1992, 1999) yet also showed here that small shifts in small-tree gbh across periods did not significantly affect our interpretations. Perturbation of the forest by the drought, therefore, had a major mixing effect enhanced by the interactions between individual tree responses to the

environmental variation directly, but also likely was the related changing competitive interactions with neighbors which themselves were affected by the drought in different ways. As an analogy following Richards (1996), we described this process more vividly as "kaleidoscopic" (Newbery and Lingenfelder 2009).

One explanatory variable repeatedly stood out with statistical significance in our new analyses, the OUI. This variable provides an important link between the small-tree class dynamics and the structure of the whole forest because it informs which species are essentially understory—almost all their trees have no larger than 50 cm gbh (a few up to 75–80 cm, Newbery et al. 1992), and which are more overstory species—those with some smaller individuals may survive and grow to >50 cm gbh and eventually reach the main canopy. All species sit along a continuum of the OUI, however. For several species, the response in relation to OUI in P_{2b} appears to be carried over into P_3. Over–understory status provides additional useful insights into tropical forest dynamics under perturbation.

Our previous work led us to show a clear species compositional forest structure, gradient and spatial pattern analysis with regard to topography (Newbery et al. 1992, 1996), and eco-physiological studies on understory tree species (Gibbons and Newbery 2003), tree species–climate and water relations analysis (Walsh and Newbery 1999), and then afterward investigations into resistance and resilience of the forest to the 1998 drought (Newbery and Lingenfelder 2004, 2009, Lingenfelder and Newbery 2009) all pointed toward an understory component that was to a large degree drought-tolerant.

However, the new results here do suggest a much more complicated picture. Some of the understory species appear to have a role in stabilizing the forest after drought perturbation but many others were destabilizing it. No trait or label can be readily ascribed to the RI_{i-j} axes in Figs. 3 and 4 because they are composed of many interrelated variables, some of which are physical and others physiological. For instance, it might be tempting to assign "water availability response" to RI_{1-2a} and "light availability response" to RI_{2a-2b} but this would be too simplistic because the growth changes are subtle and very individually tree dependent. Misleading simplifications and

over-generalization are indeed best avoided. Likewise, reaction and post-reaction phases involve responding to stress in several forms, albeit driven by declining water availability for a time, and will not be clearly independent or likely to coincide to our period boundaries for all trees (species/size/topographic location). In the same vein of thought, how is RI_{1-2b} to be interpreted? Further, stability might only be applied properly at the community level if stabilization of growth leads to stabilization of the population variables recruitment and mortality.

Whether a population stabilizes does not imply that the community as a whole is undergoing stabilization, as one species stabilizing will lead inevitably to another destabilizing. Those species that are better adapted may not show any strong response because they are resistant or tolerant, or they may be showing stabilization because they are temporarily reallocating resources as part of a strategy for better growth and survival later. In this respect, an unstable oscillation is not a "negative" reaction because under- or overcompensation means a species is showing, respectively, lowered or raised stem growth with disproportionate growth changes later, that is, possibly part of an optimal strategy in carbon allocation (Cannell and Dewar 1994, Dewar et al. 2009, Franklin et al. 2012). Alternatively, a species responds positively under stress to gain a short-term advantage but to suffer later a cost in stem growth because it either had an insufficient root system or let it be temporarily down-resourced. Becker (1990) and Grainger and Becker (2001) pointed to the large variation in root allocation (in a nutrient- and water-limited tropical forest) within and between species, suggesting highly individual responses dependent on each tree's situation.

Causes of stem growth rate change

Relative growth rate reductions in the dry period may well not be due to simple slowing of growth because one obvious resource is in temporary limiting supply and is restricting growth over the whole tree in a similar manner. Plants, and woody ones in particular, are well known to respond to changes in their environment by reallocation of resources internally, that is, reallocating resources away from stems to roots. Hence, stability is an integral and holistic measure at the

all-species (community) level. Thus, part, possibly a large part, of the explanation of reduced stem growth in P_{2a}, and a positive response in P_{2b}, is a reallocation of carbon and nutrients from stem to root growth. Farrior et al. (2013), analytically with a theoretical model, and Doughty et al. (2014), empirically from a field study in Amazonia, show that drought leads to more root growth at the cost of reduced stem growth. This would unlikely have been with a sudden switch at Danum, but as the drying enhanced (and its effects fed back on the whole tree), and with photosynthesis still operational, more carbon would have been expected to gradually flow, like a wave, toward roots as they explored the soil more widely (and competitively) in order to counteract the falling water supply. Eventually, during the very driest days and weeks, growth would have slowed over the whole tree, leaves, and fine roots shed, until rainfall re-instated the water levels and growth could resume, again first repairing lost fine roots, then in a reverse wave of allocation back to stem growth. If there was a net gain in root biomass, the extended root system might be beneficial to the re-flush in the lighted post-reaction phase with improved nutrient uptake. A trade-off in roots and stems is logically sensible because leaves are the carbon suppliers, while roots and stems are competing alternative sinks. Different species would be expected to reallocate to different degrees, depending on their size (height) and rooting depth before the dry period. Possibly then the disparate responses of species recorded in Newbery and Lingenfelder (2004, 2009), Newbery et al. (2011), and now here might be a mixed form of response, part stress/tolerance related and determined by reallocation strategies.

The understory appears to be the structural guild most affected by drought, and within these small trees, the perturbation introduced unstable oscillations in some, and stable returning responses in others. The 17 understory species need to be examined carefully (even some intermediate ones too). Do we find more tolerance for the ridge species and more reallocation for the lower-slope ones? The physiologically adapted species may be providing the stabilizing force, set against the less well-adapted species showing instability. The oscillating behavior of the many other species makes for very mixed local neighborhoods, allowing the better-adapted species to

stabilize and adapt further. Nevertheless, as much as two-month dry period is relatively short, and to have an impact over five years or so would argue for non-linear responses and feedbacks operating.

In previous analyses, four species were of particular interest because of their spatial distributions, which would suggest them well adapted to drier ridge locations: two in the understory highly clustered (*Cleistanthus contractus* and *Dimorphocalyx muricatus*), one other very common and ubiquitous (i.e., also on ridges), but not clustered in the understory (*Mallotus wrayi*), and one intermediate-storied and again clustered (*Lophopetalum beccarianum*; Appendix S1: Table S1). *Dimorphocalyx muricatus* and *M. wrayi* did respond in a marked way (Table 1, Figs. 4, 6) in being very little affected in P_{2a}, but responding strongly positively in P_{2b}, but they were not alone as *Antidesma neurocarpum* and *Magnolia candollei* also responded similarly and were not clustered or so common (Newbery et al. 1996). The other two clustered species showed no particularly special strong features in their responses, although having the same pattern as *D. muricatus* and *M. wrayi*, suggesting other reasons must explain their clustered distributions, ones unrelated to water limitation during dry periods. *Lophopetalum beccarianum* was little affected in P_{2a} and made moderate increases in RI_{i-j} to P_{2b}, but it is a larger tree on average than *D. muricatus* and *M. wrayi*: *C. contractus* suffered a reduction larger than *D. muricatus* and *M. wrayi*, and moderate increases later. It appears that *D. muricatus* and *M. wrayi* are most well adapted to the dry periods and this explains them being the two most abundant species in the plots, and of similar local high density and local dominance. The evident coriaceous leaf structure and anatomy of *D. muricatus* suggests it resists water limitation in this way, but the average leaf form of *M. wrayi*, and that its growth was slowed through possible reallocations promotes the hypothesis that it is much deeper rooted than most other small-tree species (Gibbons and Newbery 2003). For all other species, a wide mix of responses, mostly as negative reactions and weaker post-reaction responses, by being less numerous partly counterbalance the reactions of the two dominant species, and this leads to the overall, small oscillation in rgr at the whole community level.

Understanding of community dynamics

The possibility of collecting sufficiently detailed data on forest ecosystem dynamics over time to match several repeats of the full spectrum of environmental variation in the drought appears rather remote. Theoretical modeling, statistical analysis, and empirical approaches to understanding temporal stochasticity, especially in the form of colored noise (Halley 1996, Halley and Inchausti 2004), all point to the need for long time series (May 1974, 2001, Ives 1995, Ives et al. 1999). The present analysis shows that even where one moderately strong perturbation has been captured (at one location), aside from the overall stabilization of the forest, individual species varied very considerably in their growth responses. The links have still to be made between growth and population dynamics. It would presently be unwise to inductively infer that the form of response of the Danum ecosystem between 1986 and 2007 could be applied with confidence to past and future decades or centuries. Apart from not knowing whether the data to hand are at all typical or representative of a long series, it is not—perhaps cannot be—known whether any form of response will remain constant over time. There is, however, a certain propensity for the kaleidoscope to flicker in a broadly predictable way that might just allow a refined model to be tested against the next perturbation. Finally, stands the question raised in the Introduction, whether the ecosystem at Danum "reads" the redness in the environmental spectrum, and is—as a whole—"adjusted" to that stochastic noise over evolutionary time. The answer from this paper is that quite likely it is, but demonstrating this in a critically rationalist manner is very difficult.

In a broader context, incorporating reddened, rather than white, noise into thinking about and modeling how complex ecosystems function over time may be of great benefit to an understanding of many other species-rich types of vegetation. With this suggestion, however, comes the necessity of recognizing the high level of historical contingency such ecosystems must logically entail. The highly variable outcomes of past perturbation events would be expected to impinge strongly on the also highly variable outcomes of presently observed ones, making inferences about the causes of species population change, even in the short term of 10–50 yr, very difficult. Any deterministic features, like stability, are more likely to be found at an emergent level above populations, namely that of the ecosystem. By the same token, what is often referred to as complex for ecosystems, in mechanistic terms, would be better thought of as being complicated.

Literature Cited

Becker, P. 1990. Root architecture of shrubs and saplings in the understory of a tropical moist forest in lowland Panama. Biotropica 22:242–249.

Bennett, R. J., and R. J. Chorley. 1978. Environmental systems: philosophy, and analysis and control. Methuen and Co., London, UK.

Cannell, M. G. R., and R. C. Dewar. 1994. Carbon allocation in trees: a review of concepts for modeling. Advances in Ecological Research 25:59–104.

Clark, J. S. 2009. Beyond neutral science. Trends in Ecology and Evolution 24:8–15.

Clark, J. S., et al. 2010. High-dimensional coexistence based on individual variation: a synthesis of evidence. Ecological Monographs 80:569–608.

Dewar, R. C., O. Franklin, A. Makela, R. E. McMurtrie, and H. T. Valentine. 2009. Optimal function explains forest responses to global change. BioScience 59:127–139.

Doughty, C. E., Y. Malhi, A. Araujo-Murakami, D. B. Metcalfe, J. E. Silva-Espejo, et al. 2014. Allocation trade-offs dominate the response of tropical forest growth to seasonal and interannual drought. Ecology 95:2192–2201.

Farrior, C. E., R. Dybzinski, S. A. Levin, and S. W. Pacala. 2013. Competition for water and light in

closed-canopy forests: a tractable model of carbon allocation with implications for carbon sinks. American Naturalist 181:314–330.

Franklin, O., J. Johansson, R. C. Dewar, U. Dieckmann, R. E. McMurtrie, A. Brannstrom, and R. Dybzinski. 2012. Modeling carbon allocation in trees: a search for principles. Tree Physiology 32:648–666.

Gibbons, J. M., and D. M. Newbery. 2003. Drought avoidance and the effect of local topography on trees in the understory of Bornean lowland rain forest. Plant Ecology 164:1–18.

Grainger, J., and P. Becker. 2001. Root architecture and root: shoot allocation of shrubs and saplings in a Bruneian heath forest. Biotropica 33:363–368.

Halley, J. M. 1996. Ecology, evolution and 1/f-noise. Trends in Ecology and Evolution 11:33–37.

Halley, J. M., and P. Inchausti. 2004. The increasing importance of 1/f-noises as models of ecological variability. Fluctuation and Noise Letters 4: R1–R26.

Huston, M. 1979. General hypothesis of species diversity. American Naturalist 113:81–101.

Huston, M. 1994. Biological diversity: coexistence of species on changing landscapes. Cambridge University Press, Cambridge, UK.

Ives, A. R. 1995. Measuring resilience in stochastic systems. Ecological Monographs 65:217–233.

Ives, A. R., K. Gross, and J. L. Klug. 1999. Stability and variability in competitive communities. Science 286:542–544.

Legendre, P., and L. Legendre. 1998. Numerical ecology. Second edition. Elsevier, Amsterdam, The Netherlands.

Levins, R. 1968. Evolution in changing environments. Princeton University Press, Princeton, New Jersey, USA.

Levins, R. 1979. Coexistence in a variable environment. American Naturalist 114:765–783.

Lingenfelder, M., and D. M. Newbery. 2009. On the detection of dynamic responses in a drought-perturbed tropical rainforest in Borneo. Plant Ecology 201:267–290.

Loreau, M. 2010. From populations to ecosystems. Princeton University Press, Princeton, New Jersey, USA.

May, R. M. 1974. Stability and complexity in model ecosystems. Princeton University Press, Princeton, New Jersey, USA.

May, R. M. 2001. Stability and complexity in model ecosystems (new introduction to reprint). Princeton University Press, Princeton, New Jersey, USA.

Newbery, D. M., E. J. F. Campbell, Y. F. Lee, C. E. Ridsdale, and M. J. Still. 1992. Primary lowland dipterocarp forest at Danum Valley, Sabah, Malaysia: structure, relative abundance and family composition. Philosophical Transactions of the Royal Society of London B: Biological Sciences 335:341–356.

Newbery, D. M., E. J. F. Campbell, J. Proctor, and M. J. Still. 1996. Primary lowland dipterocarp forest at Danum Valley, Sabah, Malaysia. Species composition and patterns in the understorey. Vegetatio 122:193–220.

Newbery, D. M., D. N. Kennedy, G. H. Petol, L. Madani, and C. E. Ridsdale. 1999. Primary forest dynamics in lowland dipterocarp forest at Danum Valley, Sabah, Malaysia, and the role of the understory. Philosophical Transactions of the Royal Society of London B: Biological Sciences 354:1763–1782.

Newbery, D. M., and M. Lingenfelder. 2004. Resistance of a lowland rain forest to increasing drought intensity in Sabah, Borneo. Journal of Tropical Ecology 20:613–624.

Newbery, D. M., and M. Lingenfelder. 2009. Plurality of tree species responses to drought perturbation in Bornean tropical rain forest. Plant Ecology 201:147–167.

Newbery, D. M., M. Lingenfelder, K. F. Poltz, R. C. Ong, and C. E. Ridsdale. 2011. Growth responses of understory trees to drought perturbation in tropical rainforest in Borneo. Forest Ecology and Management 262:2095–2107.

Newbery, D. M., and C. E. Ridsdale. 2016. Neighbourhood abundance and small-tree survival in a lowland Bornean rainforest. Ecological Research 31: 353–366.

Newbery, D. M., and P. Stoll. 2013. Relaxation of species-specific neighborhood effects in Bornean rain forest under climatic perturbation. Ecology 94: 2838–2851.

Payne, R. W., S. A. Harding, D. A. Murray, et al. 2011. The guide to GenStat release 14, part 1: syntax and data management. Part 2: statistics. VSN International, Hemel Hempstead, UK.

Richards, P. W. 1996. The tropical rain forest: an ecological study. Second edition. Cambridge University Press, Cambridge, UK.

Roff, D. A. 2006. Introduction to computer-intensive methods of data analysis in biology. Cambridge University Press, Cambridge, UK.

Stoll, P., and D. M. Newbery. 2005. Evidence of species-specific neighborhood effects in the Dipterocarpaceae of a Bornean rain forest. Ecology 86: 3048–3062.

Tokeshi, M. 1999. Species coexistence: ecological and evolutionary perspectives. Blackwell Science, Oxford, UK.

Vanclay, J. K. 1994. Modelling forest growth and yield. CAB International, Wallingford, UK.

Walsh, R. P. D., and D. M. Newbery. 1999. The ecoclimatology of Danum, Sabah, in the context of the world's rainforest regions, with particular reference to dry periods and their impact. Philosophical Transactions of the Royal Society of London B: Biological Sciences 354:1869–1883.

Whitmore, T. C. 1984. Tropical rain forests of the Far East. Secon edition. Clarendon Press, Oxford, UK.

Supporting Information

Additional Supporting Information may be found online at: http://onlinelibrary.wiley.com/doi/10.1002/ecs2.1813/full